Draft version April 1, 2021
Typeset using LATEX **preprint** style in AASTeX631

Explorations of the BSSN formalism under spherical symmetry

Hank Chen, J. Leo Kim, and Dorsa Sadat Hosseini Khajouei

ABSTRACT

Einstein's theory of general relativity remains one of the most successful theories in modern physics to date. The governing set of Einstein Field Equations (EFEs) describe the deformation of spacetime geometry around massive objects, and yields extremely accurate predictions regarding astronomical and cosmological observations. In this report on numerical relativity, we consider the Generalized Baumgarte-Shaprio-Shibata-Nakamura (GBSSN) formulation of the EFEs (Shibata & Nakamura 1995; Baumgarte & Shapiro 1999) in spherical symmetry. Following Ref. (Brown, J. David 2008), we reproduce results and consider the effects of a scalar matter source in the GBSSN formulation. This allows us to study a collapse scenario, in which radiation falls inwards and forms a black hole, or we the in-fall of radiation into a pre-existing black hole.

1. INTRODUCTION

Einstein's theory of general relativity is one of the most successful theories of modern physics, with predictions confirmed by numerous highly-accurate measurements and observations throughout the past century. At its core, it is a *gauge theory of geometries* on a pseudo-Riemannian manifold (M, g), where g is the symmetric metric tensor. The associated Einstein Field Equations (EFEs) in natural units $G = c = 1$ read

$$\textbf{Vacuum}: \quad \mathrm{Ric}_{\mu\nu} - \frac{1}{2}\mathcal{R} = 0, \qquad \textbf{Matter}: \quad G_{\mu\nu} = 8\pi T_{\mu\nu},$$

where Ric is the *Ricci tensor*, $\mathcal{R}$ the *scalar curvature* and T the **stress-energy tensor**. A powerful result states that the *unique* (up to isometry) spherically-symmetric solution g to the vacuum EFEs is the diagonal **Schwarzchild metric**

$$g_{\mu\nu}dx^\mu dx^\nu = -(1 - \frac{2M}{r})dt^2 + \frac{dr^2}{1 - \frac{2M}{r}} + r^2 d\Omega^2, \qquad d\Omega^2 = d\theta^2 + \sin^2\theta d\phi^2, \tag{1}$$

with $d\Omega^2$ the standard metric on the unit sphere $S^2 \subset \mathbb{R}^3$. Without symmetry assumptions, however, the EFEs are are very difficult to solve, and one often must pursue numerical simulations.

By expressing the EFEs as Hamilton's equations in the **ADM Hamiltonian formalism**, it allows us to leverage first-order integration schemes to compute the time derivative at each step, instead of solving for all 4-components of the metric g at once. The ADM formalism lack long-term numerical stability, however. To amend this the **BSSN formalism** (Shibata & Nakamura 1995; Baumgarte & Shapiro 1999) introduces an auxiliary variable B that fixes the gauge, which stabilizes the Hamiltonian evolution. The **genralized BSSN (GBSSN) formalism** further relaxes the unimodularity $\det g = 1$ condition (Brown 2005; Brown, J. David 2008).

1.1. *The Generalized BSSN Formalism in Spherical Symmetry*

Given a Schwarzchild blackhole at the origin, consider a foliated embedding of spacetime $\Sigma \times \mathbb{R} \subset M \setminus \{0\}$ given by the punctured 3-space $\Sigma \cong \mathbb{R}^3 \setminus \{0\}$. The induced metric g on Σ induces in turn a **connection** Γ, and introduces the **extrinsic curvature** K of Σ. In terms of these quantities, the Hamiltonian, momentum and conformal constraints can be written

$$H = K^2 - K^{ij}K_{ij} + \mathcal{R}, \qquad P^i = \nabla_j K^{ij} - \nabla^i K, \qquad \mathcal{G}^i = \Gamma^i - g^{jk}\Gamma^i_{jk}. \tag{2}$$

Furthermore, the lapse function α and shift vector β^i satisfy the $1 + \log$ **slicing** and **Γ-driver** conditions, which ensure that the foliation Σ remains stationary under time evolution. Introduce two normalizations: the **conformal metric** γ and the **trace-free curvature** A, defined by

$$g_{ij} = e^{4\phi}\gamma_{ij} = \chi^{-1}\gamma_{ij}, \qquad K_{ij} = \chi^{-1}\left(A_{ij} + \frac{1}{3}\gamma_{ij}K\right);$$

we also denote by $\Upsilon^i = \gamma^{jk}\Upsilon^i_{jk}$ the **conformal connection** built from the conformal metric γ.

Now suppose Σ is spherically symmetric, whence γ, A become diagonal. We parameterize $\Sigma \cong \mathbb{R}^3 \setminus \{0\}$ with spheres $S^2_r \subset \mathbb{R}^3$ of radius r. Taking the ansatz

$$A_{ij} = A_{rr}\mathrm{diag}(1, -\frac{\gamma_{\theta\theta}}{\gamma_{rr}}, -\frac{\gamma_{\theta\theta}}{\gamma_{rr}}\sin^2\theta), \qquad \Upsilon^i = (\Upsilon^r \quad -\frac{\cos\theta}{\sin\theta}\gamma_{\theta\theta} \quad 0),$$

the generalized BSSN (GBSSN) equations are then expressed in terms of the state variables

$$\chi, \quad \gamma_{rr}, \quad \gamma_{\theta\theta}, \quad K, \quad A_{rr}, \quad \Upsilon^r,$$

which are all merely functions of (t, r). The GBSSN formalism under spherical symmetry (Brown, J. David 2008), involving the above state variables, shall be our main focus. To explore further than the vacuum equations, we shall also consider coupling a scalar field to the punctured evolution.

2. METHODS

2.1. *Description of numerical method*

In this section, we outline the GBSSN evolution equations and the numerical methods used to solve it. The numerical part of this project is done completely in `MATLAB`. Our state vector for time evolution is composed of a total 12 variables: the 9 parameters $\alpha, \beta^r, B^r, \chi, \gamma_{rr}, \gamma_{\theta\theta}, A_{rr}, K, \Upsilon^r$ and the 3 constraints $\mathcal{H}, \mathcal{M}_r, \mathcal{G}^r$. Primes denote the derivatives with respect to r, the GBSSN equations are given by (Brown, J. David 2008)

$$\partial_t\alpha = \beta^r\alpha' - 2\alpha K \ , \tag{3a}$$

$$\partial_t\beta^r = \frac{3}{4}B^r + \beta^r\beta^{r\prime} \ , \tag{3b}$$

$$\partial_t B^r = \partial_t\Upsilon^r + \beta^r B^{r\prime} - \beta^r\Upsilon^{r\prime} - \eta B^r \ , \tag{3c}$$

$$\partial_t\chi = \frac{2K\alpha\chi}{3} - \frac{\upsilon\beta^r{\gamma_{rr}}'\chi}{3\gamma_{rr}} - \frac{2\upsilon\beta^r{\gamma_{\theta\theta}}'\chi}{3\gamma_{\theta\theta}} - \frac{2}{3}\upsilon\beta^{r\prime}\chi + \beta^r\chi' \ , \tag{3d}$$

$$\partial_t g_{rr} = -2A_{rr}\alpha - \frac{1}{3}\upsilon\beta^r{\gamma_{rr}}' + \beta^r{\gamma_{rr}}' - \frac{2\gamma_{rr}\upsilon\beta^r{\gamma_{\theta\theta}}'}{3\gamma_{\theta\theta}} + 2\gamma_{rr}\beta^{r\prime} - \frac{2}{3}\gamma_{rr}\upsilon\beta^{r\prime} \ , \tag{3e}$$

$$\partial_t g_{\theta\theta} = \frac{A_{rr}\gamma_{\theta\theta}\alpha}{\gamma_{rr}} - \frac{\gamma_{\theta\theta}\upsilon\beta^r{\gamma_{rr}}'}{3\gamma_{rr}} - \frac{2}{3}\upsilon\beta^r{\gamma_{\theta\theta}}' + \beta^r{\gamma_{\theta\theta}}' - \frac{2}{3}\gamma_{\theta\theta}\upsilon\beta^{r\prime} \ , \tag{3f}$$

$$\begin{aligned}\partial_t A_{rr} = &-\frac{2\alpha {A_{rr}}^2}{\gamma_{rr}} + K\alpha A_{rr} - \frac{\upsilon\beta^r{\gamma_{rr}}'A_{rr}}{3\gamma_{rr}} - \frac{2\upsilon\beta^r{\gamma_{\theta\theta}}'A_{rr}}{3\gamma_{\theta\theta}} - \frac{2}{3}\upsilon\beta^{r\prime}A_{rr} + 2\beta^{r\prime}A_{rr} + \frac{2\alpha\chi\left({\gamma_{rr}}'\right)^2}{3{\gamma_{rr}}^2}\\ &-\frac{\alpha\chi\left({\gamma_{\theta\theta}}'\right)^2}{3{\gamma_{\theta\theta}}^2} - \frac{\alpha\left(\chi'\right)^2}{6\chi} - \frac{2\gamma_{rr}\alpha\chi}{3\gamma_{\theta\theta}} + \beta^r{A_{rr}}' + \frac{2}{3}\gamma_{rr}\alpha\chi\Upsilon^{r\prime} - \frac{\alpha\chi{\gamma_{rr}}'{\gamma_{\theta\theta}}'}{2\gamma_{rr}\gamma_{\theta\theta}} + \frac{\chi{\gamma_{rr}}'\alpha'}{3\gamma_{rr}}\\ &+\frac{\chi{\gamma_{\theta\theta}}'\alpha'}{3\gamma_{\theta\theta}} - \frac{\alpha{\gamma_{rr}}'\chi'}{6\gamma_{rr}} - \frac{\alpha{\gamma_{\theta\theta}}'\chi'}{6\gamma_{\theta\theta}} - \frac{2\alpha'\chi'}{3} - \frac{\alpha\chi{\gamma_{rr}}''}{3\gamma_{rr}} + \frac{\alpha\chi{\gamma_{\theta\theta}}''}{3\gamma_{\theta\theta}} - \frac{2\chi\alpha''}{3} + \frac{\alpha\chi''}{3} \ ,\end{aligned} \tag{3g}$$

$$\partial_t K = \frac{3\alpha {A_{rr}}^2}{2{\gamma_{rr}}^2} + \frac{K^2\alpha}{3} + \beta^r K' + \frac{\chi{\gamma_{rr}}'\alpha'}{2{\gamma_{rr}}^2} - \frac{\chi{\gamma_{\theta\theta}}'\alpha'}{\gamma_{rr}\gamma_{\theta\theta}} + \frac{\alpha'\chi'}{2\gamma_{rr}} - \frac{\chi\alpha''}{\gamma_{rr}} \ , \tag{3h}$$

$$\begin{aligned}\partial_t\Upsilon^r = &-\frac{\upsilon\beta^r\left({\gamma_{\theta\theta}}'\right)^2}{\gamma_{rr}{\gamma_{\theta\theta}}^2} + \frac{A_{rr}\alpha{\gamma_{\theta\theta}}'}{{\gamma_{rr}}^2\gamma_{\theta\theta}} - \frac{\upsilon\beta^{r\prime}{\gamma_{\theta\theta}}'}{3\gamma_{rr}\gamma_{\theta\theta}} + \frac{\beta^{r\prime}{\gamma_{\theta\theta}}'}{\gamma_{rr}\gamma_{\theta\theta}} + \beta^r\Upsilon^{r\prime} + \frac{A_{rr}\alpha{\gamma_{rr}}'}{{\gamma_{rr}}^3} - \frac{4\alpha K'}{3\gamma_{rr}} - \frac{2A_{rr}\alpha'}{{\gamma_{rr}}^2}\\ &+\frac{\upsilon{\gamma_{rr}}'\beta^{r\prime}}{2{\gamma_{rr}}^2} - \frac{{\gamma_{rr}}'\beta^{r\prime}}{2{\gamma_{rr}}^2} - \frac{3A_{rr}\alpha\chi'}{{\gamma_{rr}}^2\chi} + \frac{\upsilon\beta^r{\gamma_{rr}}''}{6{\gamma_{rr}}^2} + \frac{\upsilon\beta^r{\gamma_{\theta\theta}}''}{3\gamma_{rr}\gamma_{\theta\theta}} + \frac{\upsilon\beta^{r\prime\prime}}{3\gamma_{rr}} + \frac{\beta^{r\prime\prime}}{\gamma_{rr}} \ ,\end{aligned} \tag{3i}$$

where the parameter $\upsilon = 0, 1$ is a switch for the Eulerian ($\upsilon = 0$) or the Lagrangian ($\upsilon = 1$) condition. A further set of constraint evolution equations for the quantities in Eq. (2) are imposed, in order to ensure that the state variables stay on-shell throughout the evolution.

We use a fourth-order central finite difference scheme to compute the derivatives, similar to Brown, J. David (2008). This differs slightly from the exact scheme in the article, which uses a shifted finite difference stencil around the coordinate singularity at the origin with an additional guard cell. Given a variable f, the central grid fourth-order finite difference for the first order derivative is given by

$$f'(x) \approx \frac{f(x-2h) - 8f(x-h) + 8f(x+h) - f(x+2h)}{12h^2}, \tag{4}$$

and the second order derivative is given by

$$f''(x) \approx \frac{-f(x-2h) + 16f(x-h) - 30f(x) + 16f(x+h) - f(x+2h)}{12h^2}. \tag{5}$$

While normally two-level boundary conditions would be required, we instead make use of the spatial parity of our variables: we impose even parity for objects with even numbers of the index r and odd parity for objects with odd numbers of the index r. This way, for $r = 0$, we have that $f(-h) = f(h)$ and $f(-2h) = f(2h)$ for even parity quantities (such as A_{rr} or χ), and $f(-h) = -f(h)$ and $f(-2h) = -f(2h)$ for odd parity quantities (such as β^r or Υ^r).

For the temporal integration scheme, we use MATLAB's built-in `ode45` library, which is an explicit Runge-Kutta (4,5) integrator (Shampine & Reichelt 1997). To do this, we require that all of our parameters are packed into one $(12N, 1)$ state vector U, where N is the number of grid points, since `ode45` requires that the input for the time evolution is given as a column vector. Since we have 12 parameters of interest to evolve, each grid points will have 12 elements in the vector assigned to it. In our set-up, the information for the first cell is captured in `U(1:12,1)`, the information for the second cell in `U(13:24, 1)`, and so on.

2.2. *Flat spacetime initial conditions*

As an intermediate test, we check to see if the right hand side of the equations (3a)-(3i) converge to zero for a flat spacetime in spherical coordinates. The nonzero initial conditions for our flat spacetime simulation in the interval $r_{\min} = 1$ and $r_{\max} = 10$ are given by

$$\chi(0,r) = 1 \qquad \gamma_{rr}(0,r) = 1, \qquad \gamma_{\theta\theta}(0,r) = r^2, \qquad \Upsilon^r(0,r) = -\frac{2}{r}, \tag{6}$$

while all the other parameters vanish. In general relativity, given an empty universe and a flat spacetime, we expect there to be no time evolution given any initial state. To do this, we calculate the L^2 grid norm for the right hand side at a resolution h, knowing that the actual solution would just have 0 everywhere for the time derivative. The L^2 grid norm for $\frac{dU}{dt}$ in this case is given by

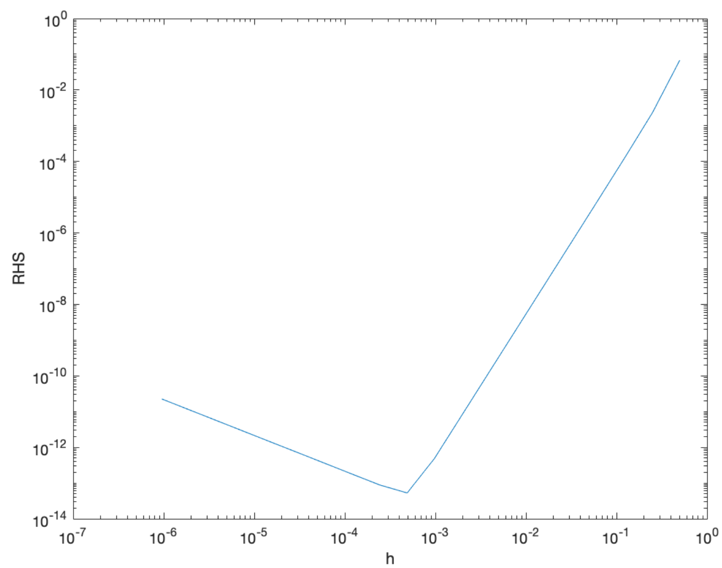

Figure 1. Convergence of RHS of equations (3a)-(3i)

$$|E^h| = \sqrt{h}\sqrt{\sum_{i=1}^{n}\left(\frac{dU_i}{dt} - 0\right)^2}. \tag{7}$$

The computation of the L^2 grid norm for the right hand side of equations (3a)-(3i) is shown in figure 1. As expected, we see fourth order convergence of the right hand side to 0 in between the regions $h \sim 1$ to $h \sim -3$. For finer resolutions, floating point error dominates.

2.3. *Puncture initial conditions*

First, for punctured evolution in spherical symmetry, we take the Schwarzchild metric Eq. (1) induced on Σ (without the dt^2 term) as the initial condition of the metric $g = \chi^{-1}\gamma$. This gives

$$\chi(0,r) = (1 + \frac{2M}{r})^{-4}, \qquad \gamma_{rr}(0,r) = 1, \qquad \gamma_{\theta\theta}(0,r) = r^2$$

for the conformal factor χ and the conformal metric γ. We also take vanishing extrinsic curvature

$$K(0,r) = 0, \qquad A_{rr}(0,r) = 0$$

as initial conditions.

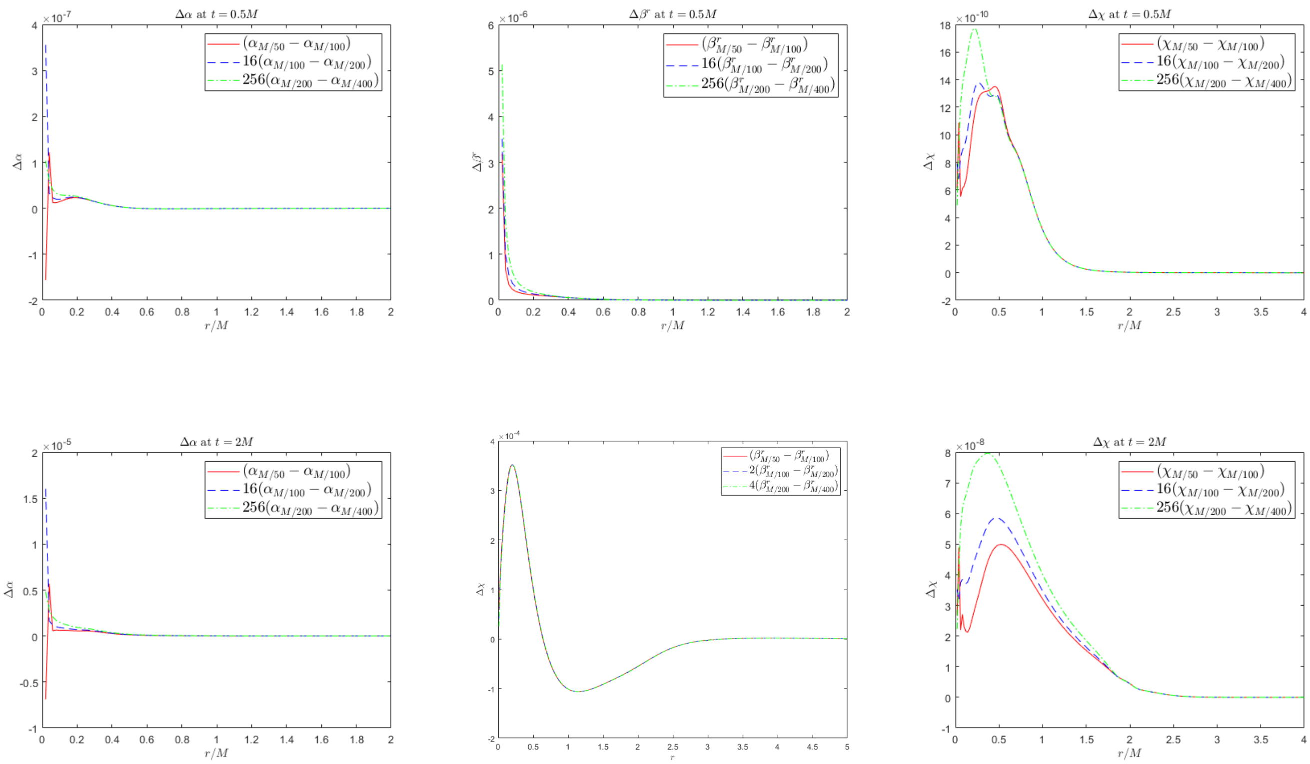

3. RESULTS

3.1. *Characteristic speeds*

3.2. *Expansion and event horizon*

A particular quantity of physical interest is the **expansion parameter** (Thornburg 2007)

$$\Theta = \nabla_i n^i + K_{ij} n^i n^j - K,$$

where n is a unit normal vector to the 3-space foliation Σ. A closed compact embedded 2-surface $\Lambda \subset \Sigma$ has $\Theta|_\Lambda = 0$ iff $K = \nabla_i n^i$ and $K_{ij} n^i n^j = 0$, hence it is locally flat with trivial extrinsic curvature. Λ is called a marginally outer trapped surface, or the **(event) horizon**, between which the curvature of spacetime changes character. It is an important quantity that detects the onset of the formation of a blackhole.

With spherical symmetry of Σ, we may write

$$\Theta = \frac{g'_{\theta\theta}}{g_{\theta\theta}\sqrt{g_{rr}}} - 2\frac{K_{\theta\theta}}{g_{\theta\theta}}$$

in terms of the physical metric g_{ij} and extrinsic curvature K_{ij}. Recall the conformal metric $g_{ij} = \chi^{-1}\gamma_{ij}$ and that $K_{\theta\theta}$ can be written in terms of $A_{\theta\theta} = -A_{rr}\frac{g_{\theta\theta}}{2g_{rr}}$ and its trace K, the expansion $\Theta = \Theta(\gamma_{rr}, \gamma_{\theta\theta}, \chi, A_{rr}, K)$ can be computed in terms of the state variables in Eqs. (3a)-(3i). By bracketing the root

$$\Theta = \Theta(t, r = r_{\text{hor}}(t)) = 0$$

at each time t, we obtain the evolution of the horizon radius $r_{\text{hor}}(t)$.

The time evolution of the expansion Θ, as well as the horizon radius r_{hor}, obtained from our numerical computations are shown in Fig. 2 below. It can be seen that, for each t, the expansion

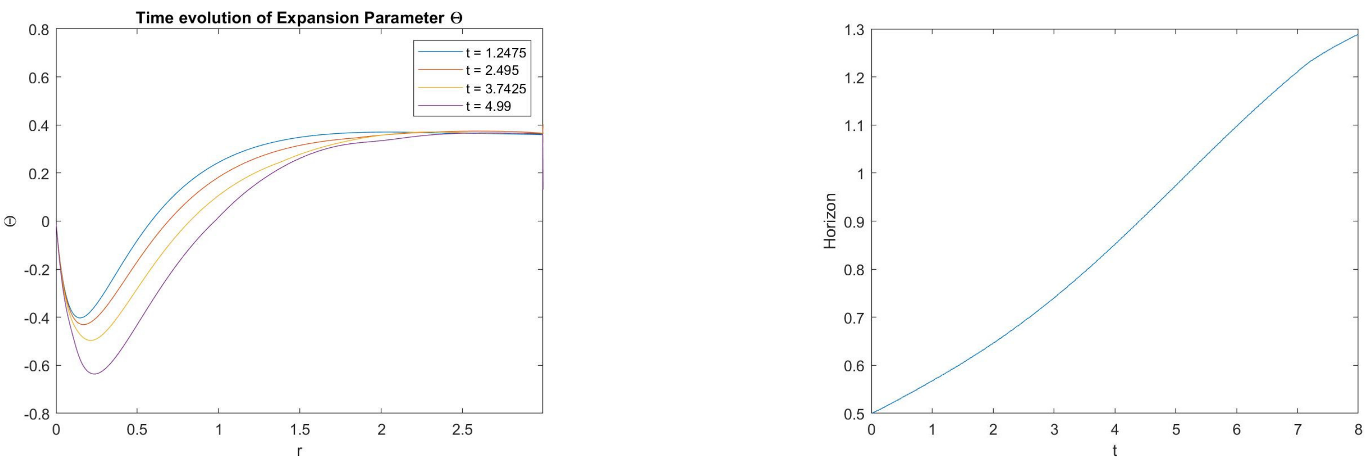

Figure 2. The expansion parameter $\Theta = \Theta(t, r)$ at times $1 < t < 5$, and the time evolution of the horizon radius $r_{\text{hor}} = r_{\text{hor}}(t)$.

achieves a global minimum and asymptotes to a steady value $\lesssim 0.4$. Furthermore, the horizon grows approximately linearly in time from $r_{\text{hor}}(0) = \frac{1}{2}$, hinting at the expansion of the blackhole horizon.

****

REFERENCES

Baumgarte, T. W., & Shapiro, S. L. 1999, Phys. Rev. D, 59, 024007, doi: 10.1103/PhysRevD.59.024007

Brown, J. D. 2005, Phys. Rev. D, 71, 104011, doi: 10.1103/PhysRevD.71.104011

Brown, J. David. 2008, Class. Quant. Grav., 25, 205004, doi: 10.1088/0264-9381/25/20/205004

Shampine, L. F., & Reichelt, M. W. 1997, SIAM Journal on Scientific Computing, 18, 1, doi: 10.1137/s1064827594276424

Shibata, M., & Nakamura, T. 1995, Phys. Rev. D, 52, 5428, doi: 10.1103/PhysRevD.52.5428

Thornburg, J. 2007, Living Rev. Rel., 10, 3. https://arxiv.org/abs/gr-qc/0512169